

New Methodology for Analytical and Optimal Design of Fuzzy PID Controllers

Baogang Hu, *Senior Member, IEEE*, George K. I. Mann, and Raymond G. Gosine, *Member, IEEE*

Abstract— This paper describes a new methodology for the systematic design of fuzzy PID controllers based on theoretical fuzzy analysis and genetic-based optimization. An important feature of the proposed controller is its simple structure. It uses a one-input fuzzy inference with three rules and at most six tuning parameters. A closed-form solution for the control action is defined in terms of the nonlinear tuning parameters. The nonlinear proportional gain is explicitly derived in the error domain. A *conservative design strategy* is proposed for realizing a guaranteed-PID-performance (GPP) fuzzy controller. This strategy suggests that a fuzzy PID controller should be able to produce a linear function from its nonlinearity tuning of the system. The proposed PID system is able to produce a close approximation of a linear function for approximating the GPP system. This GPP system, incorporating with a genetic solver for the optimization, will provide the performance no worse than the corresponding linear controller with respect to the specific performance criteria (i.e., response error, stability, or robustness). Two indexes, linearity approximation index (LAI) and nonlinearity variation index (NVI), are suggested for evaluating the nonlinear design of fuzzy controllers. The proposed control system has been applied to several first-order, second-order, and fifth-order processes. Simulation results show that the proposed fuzzy PID controller produces superior control performance than the conventional PID controllers, particularly in handling nonlinearities due to time delay and saturation.

Index Terms— Fuzzy logic control, genetic algorithms, nonlinear control, optimal control, PID control.

I. INTRODUCTION

FUZZY logic control (FLC) technique has found many successful industrial applications and demonstrated significant performance improvements [7], [9], [12], [18], [35]. However, fuzzy controller design remains a fuzzy process due to the fact that there is insufficient analytical design technique in contrast with the well-developed linear control theories. Although the functions of fuzzy systems have the advantage of being relatively easy to understand, the systems become complex or nontransparent due to many design parameters involved. Considering fuzzy PID-like controllers, we summarize the design parameters within two groups: structural parameters and tuning parameters (Table I). While

the structural parameters are determined during off-line design, tuning parameters can be calculated during on-line adjustments of the controller to enhance the process performance, as well as to accommodate the adaptive capability to system uncertainty and process disturbance. Some parameters can be called either structural or tuning parameters depending on their usage. The optional design parameters are marked by an asterisk (*) in Table I.

A wide variety of fuzzy PID-like controllers have been developed. Only a few of the designs are listed in Table II to highlight the significant differences in the design parameters and structures. In most cases, fuzzy controller design is accomplished by trial-and-error methods using computer simulations. Significant studies based on the closed-form analysis of fuzzy PID-like controllers started with the work of Ying, Siler, and Buckley [34], [39], [40], where they have used a simple four-rule controller similar to that of Murakami and Maeda [28]. More analytical work in this regard was subsequently reported for the four-rule controllers [6], [23], [38], and linear-like fuzzy controllers [3], [5]. Palm has analytically demonstrated the equivalence between the fuzzy controller and sliding-mode controllers [29]. It is possible to build a fuzzy controller which provides better performance than a conventional PID controller, but a fundamental question remains—*Is a fuzzy PID controller guaranteed to outperform a conventional PID controller for any type of process?* It has been reported that a specific fuzzy controller is not necessarily better than a conventional PI controller [5]. This raises another question—*Under what conditions can a fuzzy PID system provide better performance than a linear PID controller?* To date, no satisfactory formal techniques have been developed to solve these problems. Moreover, in a study of optimal design for fuzzy controllers, two relationships must be established: 1) design parameters and control nonlinearity, and 2) control nonlinearity and process performance.

This work is an attempt to undertake the development of a new analytical approach to the optimal design of fuzzy controllers. We propose a new methodology for the optimal design of fuzzy PID controllers. While an analytically based study is conducted for the first relationship, the second relationship is solved by using a genetic method. A simple controller applying a single variable, three rules, and six design parameters is developed. The properties of the control action are discussed in terms of the design parameters. The nonlinear proportional gain is explicitly derived in an error domain. The issues of nonlinear controller design are discussed, and a conservative design strategy is suggested for a guaranteed-PID-performance

Manuscript received January 30, 1997; revised May 26, 1999. This work was supported in part by Natural Sciences and Engineering Research Council of Canada, the Canadian Space Agency, Petro-Canada Resources, and Chinese National Science Foundation under Grant 69 874 041.

B. Hu is with National Laboratory of Pattern Recognition, Institute of Automation, Chinese Academic of Science, Beijing, 100080 R.O.C.

G. K. I. Mann and R. G. Gosine are with C-CORE and the Faculty of Engineering and Applied Science, Memorial University of Newfoundland, St. John's, A1B 3X5 Canada.

Publisher Item Identifier S 1063-6706(99)08257-0.

TABLE I
DESIGN PARAMETERS OF A FUZZY PID CONTROLLER. (* OPTIONAL DESIGN PARAMETERS)

Design Parameters	
Structural Parameters	Tuning Parameters
Input variables to fuzzy inference	Proportional gain (K_p)
Output variables of fuzzy inference	Integral gain (K_I)
Fuzzy linguistic sets	Derivative gain (K_D)
Membership functions (MFs)	Parameters of MFs
Fuzzy rules	Scaling factors (SFs)
Inference mechanisms (IMs)	Parameters for switching knowledge-based systems*
Defuzzification mechanisms (DMs)	Parameters of DMs or Look-up tables (LTs)*
PID connective structures	Parameters for switching control schemes*
Anti-windup structures*	Parameters for anti-windup*

TABLE II
COMPARISON OF FUZZY PID-LIKE CONTROLLERS. (NOTE: SOME DESIGN PARAMETERS MIGHT BE APPLIED BUT NOT GIVEN IN THE REFERENCES. MF's = MEMBERSHIP FUNCTIONS, RM = RELATION MATRIX)

Controller Type	Input Variables	Number of Rules	Required Parameters	Source of Reference
PI	$e, \Delta e$	48	$s_e, s_{\Delta e}, s_u$	[24]
Self-organizing PI	$e, \Delta e$	24 - 45	$s_e, s_{\Delta e}, s_u$	[32]
PI-A	$e, \Sigma e$	49	$s_e, s_{\Sigma e}, s_u$	[4]
PI-B	$e, \Delta e$	49	$s_e, s_{\Delta e}, s_u$	
Self-regulating PI, PID	$e, \Delta e$	49, 343	$s_e, s_{\Delta e}, s_u, k_D, k_I$	[31]
Two-stage PI	$e, \Delta e$	25	$e_{switch}, \Delta e_{switch}$	[20]
Model-based	$e, \Delta u$	> 49	$s_{\Delta e}, s_{\Delta u}$	[11]
PI	$e, \Delta e$	4	K_p, K_I, L	[39,40]
P	Δe	7	Δe_{range}	[26]
PI	$e, \Delta e$	9	$e_{range}, \Delta e_{range}$	
Adaptive network	$\theta, \Delta \theta$	4	$\theta_{min}, \theta_{max}, \Delta \theta_{min}, \theta_{max}$ 12 for MFs	[15]
Resetting PI	e, u	98	$s_e, s_{\Delta e}, s_u, s_{\Delta u}, p$	[19]
Gain-scheduling PID	$e, \Delta e$	147	$K_{p,min}, K_{p,max}, K_{D,min}, K_{D,max}$	[41]
PID Types 1-5	$e, \Delta e$	49 - 56	-	[12]
Self-tuning	$e, \Delta e$	49	K_u, t_u, γ	[14]
Sliding-mode PD	s_{pN}, d_N	8	λ, N_e	[29]
Multi-region PI	$\Delta V, e, \Delta e, \Delta u$	50	$K_p, T_D, s_e, s_{\Delta e}, s_{\Delta u}$	[33]
PD	$e_s, \Delta e_s$	4	K_p, K_D, K_U, L	[23]
Genetic fuzzy model	I	6	$I_{max}, N_{min}, N_{max}$ 30 for RM, 12 for MFs	[30]
Optimal PI	$e, \Delta e$	25	8 for MFs	[25]
Genetic fuzzy net	$e, \Delta e$	9 or 25	9 or 25 for MFs	[17]

fuzzy controller. Two indexes are proposed for the evaluation of nonlinear controller designs. For an optimal system design using genetic algorithms, an overall performance index is proposed including several individual performance indexes. Finally, numerical studies are performed on several processes including nonlinearities due to time delay and saturation.

II. NEW METHODOLOGY

A new methodology is proposed for the analytical design of a fuzzy PID controller. Fig. 1 shows the proposed methodology with respect to the data or parameter flow in off-line design. In Step 1, the structure of a fuzzy PID controller is

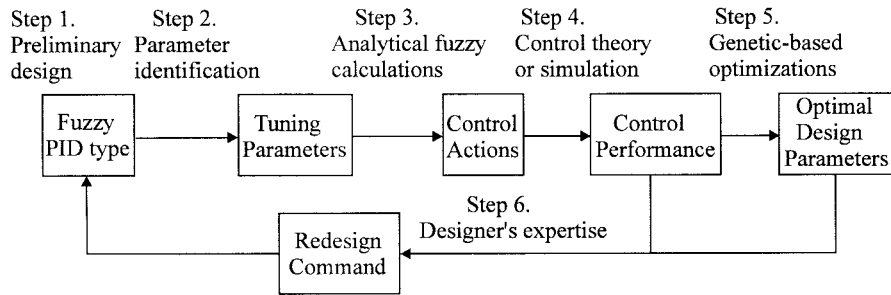


Fig. 1. Proposed methodology with respect to the data or parameter flows for optimal design of fuzzy PID controllers.

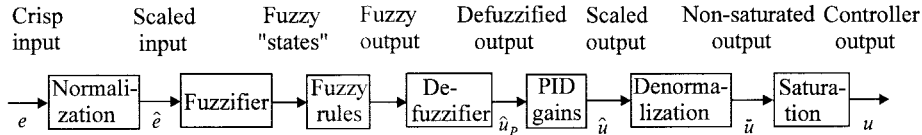


Fig. 2. Structure of the proposed fuzzy PID controller.

designed and the structural parameters are set for the preliminary design. The tuning parameters are identified in Step 2, while in Step 3 an analytical fuzzy calculation is performed, which produces a closed-form relationship between the design parameters and control action for the fuzzy inference. In Step 4, numerical simulation (or control theory) is used to obtain the control performance data. In Step 5, genetic-based optimizations are carried out to produce optimal design parameters. This also provides useful information for the redesign of the original system. Finally, if necessary, redesign is undertaken using the designer's expertise for further improvement to the control system. Note that the theoretical study in Step 3 makes the fuzzy controller transparent. This step is important since it will establish a close link between fuzzy control design technique and classical/modern control theory.

Simplicity is a key principle of this design methodology. The reason is obvious if we see that fuzzy logic controllers are systems which simulate human control exercise. For many everyday control tasks, people initially try to apply simple rules. Three rules used in this work are very common in a feedback set-point control problem. If a satisfactory control process can be achieved by applying simple rules, the use of complex rules, which is often associated with a higher cost of computation, becomes unnecessary. Simplicity is the best and direct way to maintain a clearly physical insight into the control laws. It also makes high-dimensional fuzzy systems tractable for using simple mathematical expressions for describing functionality between design parameters and nonlinearity. The simplicity of a system can be assessed by examining the structure of the information flow and the total number of design parameters. It is preferable for a system to include high modularity, parallelism, concurrency, and normality for implementation in both software and hardware. To simulate the simplest control exercise of human beings, we develop a one-input/three-rule fuzzy PID controller associated with at most six design parameters. This system, having a simple structure to form a control curve, is closely analogous to a linear PID controller.

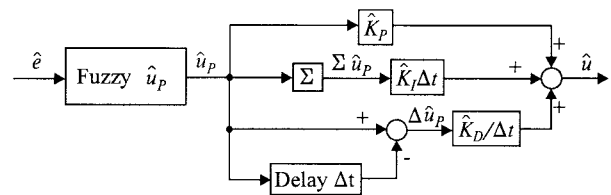


Fig. 3. A single input fuzzy PID controller.

III. STRUCTURE OF FUZZY PID CONTROLLER

Compatible with the cascade structure of a conventional PID controller, a one-input fuzzy PID controller is proposed (Fig. 2). An error signal is defined by $e(n) = r(n) - y(n)$; with $r(n)$ being a reference input, and $y(n)$ a plant response at time instant n . The controller output (or, control input to a plant) is denoted by $u(n)$. The scaled discrete-time output $\hat{u}(n)$ is the sum of three terms (Fig. 3), represented by

$$\hat{u}(n) = \hat{K}_P \hat{u}_P(n) + \hat{K}_I \sum_{i=0}^n \hat{u}_P(i) \Delta t + \hat{K}_D \frac{\Delta \hat{u}_P(n)}{\Delta t}, \quad n = 0, 1, 2, \dots \quad (1)$$

where we define \hat{u}_P as a defuzzified proportional output; and its change is $\Delta \hat{u}_P$ ($\Delta \hat{u}_P(0) = 0$) for the sampling period, Δt . \hat{K}_P , \hat{K}_I , and \hat{K}_D are the normalized proportional, integral, and derivative gains, respectively. They are all normalized within a range of $[0, 1]$. Three rules used for the fuzzy control are

- R1: if (\hat{e} is NB) then (\hat{u}_P is NB)
 - R2: if (\hat{e} is PB) then (\hat{u}_P is PB)
 - R3: if (\hat{e} is AZ) then (\hat{u}_P is AZ)
- (2)

where \hat{e} is the scaled error signal. The fuzzy variable "NB" stands for "negative big", "PB" for "positive big" and "AZ" for "approximate zero". The membership functions for \hat{e} and \hat{u}_P are shown in Fig. 4. For simplicity, we use triangular membership functions. While the membership functions for \hat{e} are fixed, the membership functions for \hat{u}_P may change according

TABLE III
PARAMETERS FOR THE PROPOSED OPTIMAL FUZZY AND OPTIMAL LINEAR PID-TYPE CONTROLLERS

PID type	Parameters	
	Optimal Fuzzy	Optimal Linear
PID	$\hat{K}_P, \hat{K}_I, \hat{K}_D, s_u, x_1, x_2$	$\hat{K}_P, \hat{K}_I, \hat{K}_D, s_u$
PD	$\hat{K}_P, \hat{K}_D, s_u, x_1, x_2$	$\hat{K}_P, \hat{K}_D, s_u$
PI	\hat{K}_I, s_u, x_1, x_2	\hat{K}_I, s_u

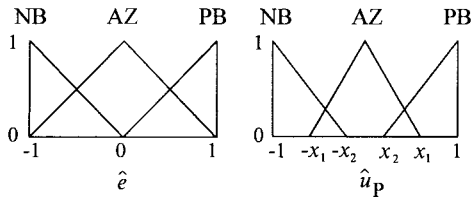


Fig. 4. Membership functions of a three-rule fuzzy controller.

to the parameters x_1 and x_2 , which will be discussed in the next section. For a set-point process control, we normalize the crisp input data $e(n)$ into scaled data $\hat{e}(n)$ using the following transformation:

$$\hat{e}(n) = \begin{cases} 1, & s_e e(n) > 1 \\ s_e e(n), & |s_e e(n)| \leq 1 \\ -1, & s_e e(n) < -1. \end{cases} \quad (3a)$$

Two operations are performed in the normalization. The scaling factor s_e is calculated as

$$s_e = |1/[r(0) - y(0)]| = |1/e(0)| \quad (3b)$$

where $r(0)$ and $y(0)$ are the initial values of reference input and response ($r(0) - y(0) \neq 0$), respectively. The second operation is a saturation function as expressed by (3a). We have noted that the selection of a universe of discourse is usually arbitrary; this may cause an additional complexity in the selection of the scaling factor. The saturation operation in (3a) provides a standard calculation of s_e . The normalized error \hat{e} falls within the range $[-1, 1]$. Denormalization of the scaled output \hat{u} is expressed in the form

$$\bar{u}(n) = s_u \hat{u}(n) \quad (4)$$

where $\bar{u}(n)$ is a crisp output without saturation operation, and s_u is a denormalized factor.

Saturation is considered in the control structure (Fig. 2) for true control action analysis. The final controller output is

$$u(n) = \begin{cases} u_{\max}(n), & \bar{u}(n) > u_{\max} \\ \hat{u}(n), & u_{\min} \leq \bar{u}(n) \leq u_{\max} \\ u_{\min}(n), & \bar{u}(n) < u_{\min} \end{cases} \quad (5)$$

where u_{\min} and u_{\max} are the minimum and maximum allowable inputs to the plant.

IV. IDENTIFICATION OF DESIGN PARAMETERS

In this work, as few parameters as possible are included. The first two tuning parameters are associated with the allocation of membership functions for \hat{u}_P (Fig. 4), where x_1 is associated

with ‘‘AZ,’’ and x_2 with ‘‘PB’’ and ‘‘NB.’’ Each parameter changes the width of the associated triangular membership function. For effective application of tuning parameters from a fixed number of design parameters, we suggest assigning them to consequent fuzzy sets rather than to antecedent fuzzy sets. Otherwise, the undesired output may result when no rule or a single rule fires (refer to ‘‘rule completeness’’ in [9]).

For a conventional (or linear) PID controller, the gains K_P , K_I , and K_D are independent tuning parameters. Without *a priori* knowledge, they could take any nonnegative value. This arbitrary range usually causes trouble in determining the universe of discourse of the gains in a fuzzy PID controller design. In order to avoid this difficulty, we propose applying the normalized control gains denoted in (1). An additional parameter, s_u , is used to scale the overall values of the gains. The universe of discourse of this parameter can be easily obtained from the maximum absolute value of $u(n)$. Therefore, a total of six tuning parameters for the generalized fuzzy PID controller is included in the system. The range for each design variable is given by

$$\begin{aligned} 0 < \hat{K}_P \leq 1 & \quad 0 \leq \hat{K}_I \leq 1 & \quad 0 \leq \hat{K}_D \leq 1 \\ 0 < s_u \leq \max(|u_{\min}|, |u_{\max}|) & \quad 0 < x_1 \leq 1 & \quad (6) \\ & \quad 0 \leq x_2 < 1. \end{aligned}$$

Three normalized gains, \hat{K}_P , \hat{K}_I , and \hat{K}_D , together with the output scale factor s_u are interdependent. The reason for adding s_u is to provide a standard approach in the controller design.

As a generalized method, this three-gain fuzzy PID controller is ready to change into a two-gain fuzzy PI or PD controller. At least one parameter can be eliminated for the two-gain controller. If a fuzzy PI controller is selected for use, only four independent tuning parameters are employed for the condition suggested in [37]

$$K_I/K_P < 1. \quad (7)$$

Based on this *a priori* knowledge, we remove \hat{K}_P as a variable and define it as a unity; i.e., $\hat{K}_P = 1$. Table III lists the tuning parameters for the optimal fuzzy PID-type as well as optimal linear PID-type controllers proposed in this work. Note that the normalization technique is also applied to a linear PID controller (Table III).

V. ANALYTICAL FUZZY CALCULATIONS

In this fuzzy PID controller, we apply the ‘‘max-min-gravity’’ fuzzy reasoning method, known as Zadeh–Mamdani’s

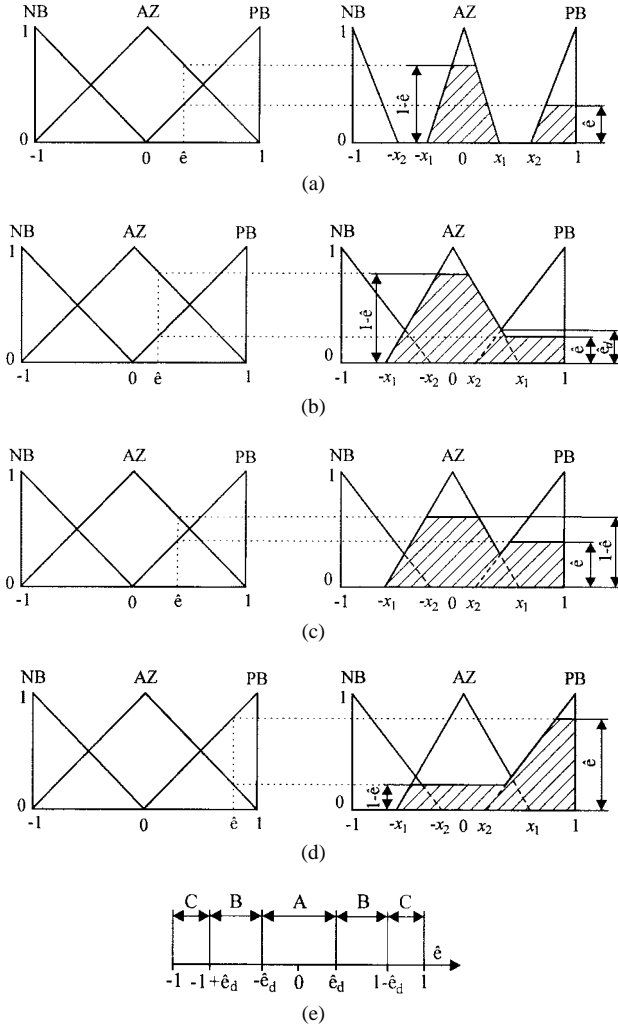


Fig. 5. Two cases for fuzzy output aggregation. (a) Case 1: $x_1 \leq x_2$. (b) Case 2: $x_1 > x_2$. Range A: $0 \leq |\hat{e}| \leq \hat{e}_d$. (c) Case 2: $x_1 > x_2$. Range B: $\hat{e}_d < |\hat{e}| \leq 1 - \hat{e}_d$. (d) Case 2: $x_1 > x_2$. Range C: $1 - \hat{e}_d < |\hat{e}| \leq 1$. (e) Case 2: $x_1 > x_2$. Three ranges with respect to \hat{e} .

method. The hatched areas in Fig. 5 represent the combination of consequents of each rule, or aggregation, in the fuzzy inference system. The center of area method (COA) is used as the defuzzification procedure [7]

$$\hat{e} = \frac{\left[\int_{c \in S} c_i \mu_c(c) dc \right]}{\left[\int_{c \in S} \mu_c(c) dc \right]} \quad (8)$$

where \hat{e} is the defuzzified control action, and μ_c is the membership function of a control inference with its support set given by

$$S = \{c \mid \mu_c(c) > 0\}. \quad (9)$$

Two cases are given for the defuzzification. While Case 1 [Fig. 5(a)] has two separated areas due to its nonoverlapping adjacent membership functions, a continuous area results in Case 2 because of the overlapping of the adjacent membership functions [Fig. 5(b)–(d)]. In Case 2, three ranges [Fig. 5(e)] are distinguished with respect to \hat{e} for derivation of the defuzzified output. The three different ranges are determined by \hat{e}_d (which point is called *division point*)

$$\hat{e}_d = (x_1 - x_2) / (1 + x_1 - x_2). \quad (10)$$

In fact, this value is also equal to the height of the crossing point between two adjacent membership functions of the consequent fuzzy sets [Fig. 5(b)]. The following expressions have been derived for the defuzzified output \hat{u}_P by taking the center of the hatched area(s). For convenience, the time instant notation n is dropped for both \hat{u}_P and \hat{e} .

Case 1 (Nonoverlapping): $x_1 \leq x_2$

$$\hat{u}_P = \frac{y_2 \hat{e} [3x_2(2 - |\hat{e}|) + y_2(3 - \hat{e}^2)]}{3[2x_1(1 - \hat{e}^2) + y_2(2|\hat{e}| - \hat{e}^2)]}. \quad (11a)$$

Case 2 (Overlapping): $x_1 > x_2$

Range A: $0 \leq |\hat{e}| \leq \hat{e}_d$

$$\hat{u}_P = \frac{\hat{e} [3(1 - x_1^2) + 3x_1^2|\hat{e}| - x_1^2\hat{e}^2]}{3[2x_1 + 2(1 - x_1)|\hat{e}| - x_1\hat{e}^2]}. \quad (11b)$$

Range B: $\hat{e}_d < |\hat{e}| < 1 - \hat{e}_d$

$$\hat{u}_P = \frac{\hat{e} \{y_2|\hat{e}| [3x_2(2 - |\hat{e}|) + y_2(3 - \hat{e}^2)] - y_1\hat{e}_d [(3 - \hat{e}_d)x_1 - y_1]\}}{3|\hat{e}| [2x_1(1 - \hat{e}^2) + y_2(2|\hat{e}| - \hat{e}^2) - y_1\hat{e}_d]}. \quad (11c)$$

Range C: $1 - \hat{e}_d \leq |\hat{e}| \leq 1$

$$\hat{u}_P = \frac{\hat{e} \{z_1 [3 - x_1^2(1 + |\hat{e}| + \hat{e}^2)] - y_2z_3 [3 - y_2(1 - |\hat{e}| + \hat{e}^2)]\}}{3|\hat{e}| [z_1(2 + x_1z_2) - y_2z_3]}. \quad (11d)$$

in which the intermediate variables are defined as

$$\begin{aligned} z_1 &= 1 - |\hat{e}| & z_2 &= 1 + |\hat{e}| & z_3 &= 1 - 2|\hat{e}|, \\ y_1 &= x_1 - x_2 & y_2 &= 1 - x_2. \end{aligned} \quad (11e)$$

VI. COMPARISON BETWEEN FUZZY PID AND CONVENTIONAL PID CONTROLLERS

Equation (11) gives a closed-form solution to the proposed fuzzy proportional action. Further analysis of the fuzzy PID gains compared to a conventional cascade PID controller can be made. The present linear PID controller in its digital form is represented as

$$u(n) = K_P e(n) + K_I \sum_{i=0}^n e(i) \Delta t + K_D \frac{\Delta e(n)}{\Delta t}, \quad n = 0, 1, 2, \dots \quad (12)$$

where K_P , K_I , and K_D are constant gains, and we impose the initial condition $\Delta e(0) = 0$. Analogous to above, nonlinear PID gains can be obtained for the fuzzy PID controller. Rewriting (1), we get

$$\begin{aligned} \hat{u} &= \left(\hat{K}_P \frac{\hat{u}_P}{\hat{e}} \right) \hat{e} + \left(\hat{K}_I \frac{\sum \hat{u}_P}{\sum \hat{e}} \right) \sum \hat{e} \Delta t + \left(\hat{K}_D \frac{\Delta \hat{u}_P}{\Delta \hat{e}} \right) \frac{\Delta \hat{e}}{\Delta t} \\ &= (K_P)_{\text{eq}} \hat{e} + (K_I)_{\text{eq}} \sum \hat{e} \Delta t + (K_D)_{\text{eq}} \frac{\Delta \hat{e}}{\Delta t} \end{aligned} \quad (13)$$

where we define $(K_P)_{\text{eq}}$, $(K_I)_{\text{eq}}$, and $(K_D)_{\text{eq}}$ to be the *equivalent* proportional, integral, and derivative gains to a conventional PID controller, respectively. Note that the scalar s_u is not included for the equivalence since this factor does not change the nonlinear behavior of the controllers. The equivalent proportional and derivative gains are readily found

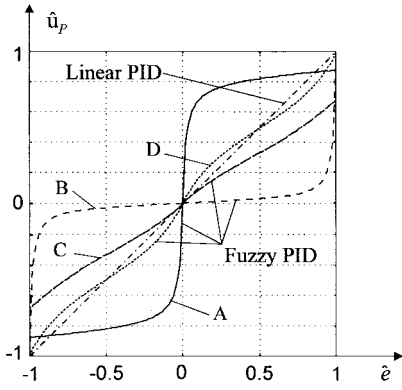


Fig. 6. “ \hat{e} versus \hat{u}_P ” plots of linear and fuzzy PID controllers. A: $x_1 = 0.0079$, $x_2 = 0.630$. B: $x_1 = 0.874$, $x_2 = 0.945$. C: $x_1 = 0.466$, $x_2 = 0$. D: $x_1 = \epsilon(2 - \epsilon)/4$, $x_2 = 1 - \epsilon$ (ϵ , an arbitrarily small value, >0).

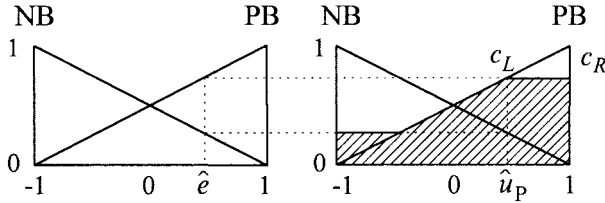


Fig. 7. Membership functions of a two-rule fuzzy controller.

from (11) and (13). However, the equivalent integral gain can be explicitly obtained only when \hat{e} is a known function with respect to time.

A conventional PID controller can be implemented using a simple fuzzy controller. Fig. 6 shows different “ \hat{u}_P versus \hat{e} ” plots describing linear and fuzzy PID controllers. If a plot shows a linear relationship

$$\hat{u}_P(n) = \hat{e}(n) \quad (14)$$

a linear PID controller can be constructed by substituting this relationship into (13). Using rules of R1 and R2 in (2) with the membership functions shown in Fig. 7, we realize a linear relationship using the smallest of maximum (SOM) defuzzification method [16]. This method is a simplified version of the mean of maxima (MOM) defuzzification method [7]. Instead of finding the mean point of all c_j , where c_j is an element giving the maximal grade of membership in (9b), the SOM is selected as the point that corresponds to the shortest distance to the origin (Fig. 7)

$$\hat{e} = \begin{cases} c_L, & \text{such that } \min(|c_L|, |c_R|) = |c_L| \\ c_R, & \text{such that } \min(|c_L|, |c_R|) = |c_R| \end{cases} \quad (15)$$

where c_L and c_R are the left and right points of c_j . This two-rule fuzzy PID-type controller using SOM defuzzification will result in a linear PID controller. For this linear realization, an infinite number of rules have to be used for linear-like fuzzy controllers in [3], [5], and [40] by using the COA defuzzification method. It is reported in [27] that, using the product-sum-gravity reasoning method, linear PD controllers have been realized by four rules and linear PID controllers by eight rules.

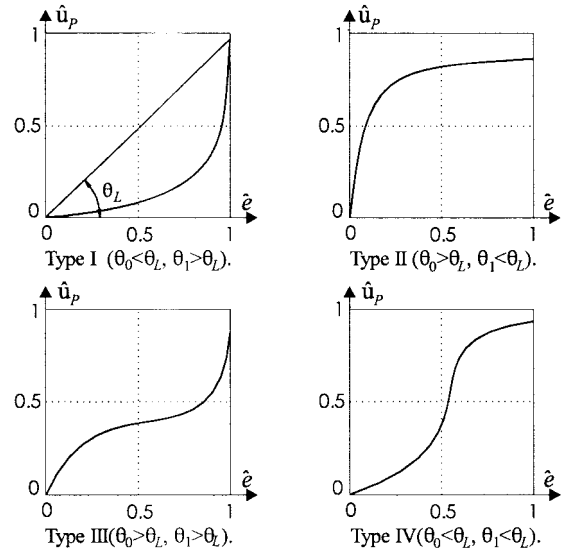


Fig. 8. Four types of simple nonlinear curves. θ_L : angle corresponding to fitting a linear function. (a) Type I ($\theta_0 < \theta_L, \theta_1 > \theta_L$). (b) Type II ($\theta_0 > \theta_L, \theta_1 < \theta_L$). (c) Type III ($\theta_0 > \theta_L, \theta_1 > \theta_L$). (d) Type IV ($\theta_0 < \theta_L, \theta_1 < \theta_L$).

VII. PROPERTIES OF FUZZY PROPORTIONAL ACTIONS

In this section, we will discuss properties of the proportional action, $\hat{u}_P(\hat{e}, x_1, x_2)$, in error domains. The nonlinearities of the present three-rule fuzzy PID controller are produced by two design parameters: x_1 and x_2 . We call them “nonlinear tuning parameters.” The analysis of fuzzy proportional actions is essential because the actions are a direct output from the fuzzy inference, and they also influence the fuzzy integral and derivative actions. Several properties of the relationship between \hat{u}_P and \hat{e} are summarized below to provide some useful design guidelines for fuzzy PID controller design.

- 1) $|\hat{u}_P| \leq 1$ limits the magnitude of normalized proportional action to be less than or equal to one.
- 2) $\hat{u}_P(\hat{e} = 0) = 0$ is a necessary condition for a zero steady-state error.
- 3) $|\hat{u}_P(\hat{e} = \pm 1)| = \max(|\hat{u}_P|) = (2 + x_2)/3$ indicates a maximum proportional controller output for a fast rise-up response when error is at an extreme. (Note that \hat{u}_P is not totally normalized because of $\max(|\hat{u}_P|) \leq 1$).
- 4) $\hat{u}_P(\hat{e})$ is a continuous function with respect to \hat{e} .
- 5) $\hat{u}_P(\hat{e})$ provides a monotonic proportional action with respect to \hat{e} . It presents a nonlinear, one-to-one, mapping relationship between \hat{e} and \hat{u}_P .
- 6) $\hat{u}_P(\hat{e}) = -\hat{u}_P(-\hat{e})$ gives an antisymmetric proportional control action with respect to \hat{e} .
- 7) $\hat{u}_P(\hat{e})$ can form three types (Type I, II, and III) of nonlinear (or control) curves shown in Fig. 8.
- 8) $\hat{u}_P(\hat{e})$ cannot exhibit a linear function. A close approximation of the linear relationship (Curve C in Fig. 6) is obtained when $x_1 = 0.466$ and $x_2 = 0$.
- 9) $\partial \hat{u}_P / \partial \hat{e} > 0$. The slope for the function $\hat{u}_P(\hat{e})$ is always positive. This indicates that there is no flat zones ($\partial \hat{u}_P / \partial \hat{e} = 0$) in the control curve.
- 10) $\partial \hat{u}_P / \partial \hat{e}$ can be viewed as a Normalized Sensitivity (NS) function. The higher the value, the more sensitive the

controller to error. Note that for a linear PID controller, $\partial \hat{u}_P / \partial \hat{e} = 1$. This function can be used to compare the normalized sensitivities of fuzzy PID and linear PID controllers. A complete sensitivity comparison should include the proportional gain and denormalized factors.

- 11) For the overlapping case (Case 2), the normalized sensitivity at the zero error point (NS_0) is controlled by x_1 (16). In the nonoverlapping case (Case 1), NS_0 is the function of both x_1 and x_2 .

$$NS_0 = \left. \frac{\partial \hat{u}_P}{\partial \hat{e}} \right|_{\hat{e}=0} = \begin{cases} \frac{1-x_2^2}{2x_1}, & x_1 \leq x_2 \\ \frac{1-x_1^2}{2x_1}, & x_1 > x_2. \end{cases} \quad (16)$$

- 12) Both x_1 and x_2 , in (17), can affect the sensitivity (NS_1) at the extreme error points.

$$NS_1 = \left. \frac{\partial \hat{u}_P}{\partial \hat{e}} \right|_{\hat{e}=\pm 1} = \begin{cases} \frac{4x_1(2+x_2)}{3(1-x_2)}, & x_1 \leq x_2 \\ \frac{(x_1+x_2)(3x_1-x_2+4)}{3(1-x_2)}, & x_1 > x_2. \end{cases} \quad (17)$$

- 13) The sensitivity variations for NS_0 and NS_1 are partially interdependent. Suppose NS_0 is any given value within the range from 0 to ∞ , i.e., $[0, \infty)$. Then, the limited ranges for NS_1 are

$$\begin{cases} \left[\frac{2z_0(2z_0+4)}{3(1-z_0)}, \frac{4}{NS_0} \right), & (NS_0 \neq 0), \quad x_1 \leq x_2 \\ \left[\frac{z_0(3z_0+4)}{3}, \frac{2z_0(2z_0+4)}{3(1-z_0)} \right], & (z_0 \neq 1), \quad x_1 > x_2 \end{cases} \quad (18a)$$

where

$$z_0 = \sqrt{1 + NS_0^2} - NS_0. \quad (18b)$$

Thus the variations in NS_0 and NS_1 at the two extreme points are

$$\begin{aligned} NS_0 = 0, \quad NS_1 \text{'s range} &= [7/3, \infty), & \text{when } x_1 = 1 \\ NS_0 = \infty, \quad NS_1 = 0, & & \text{when } x_1 \rightarrow 0. \end{aligned} \quad (19)$$

The significant feature of the proposed controller is the application of a single-input scheme, e , to evaluate the fuzzy proportional action. Most other researchers have used the two-input scheme (Table II), e and Δe , to produce the coupled PD actions, or coupled PI actions by two-to-one mappings. Due to this coupling effect, the change of error Δe will also alter the proportional action which may amplify any spurious signal or noise significantly. Therefore, the present controller has less sensitivity to the noisy data than a conventional two-input fuzzy controller.

VIII. NONLINEAR CONTROLLER DESIGN AND CONSERVATIVE DESIGN STRATEGY

Fig. 6 demonstrates that the fuzzy PID controller is a nonlinear system. Therefore, three issues are related to the design of

the system: 1) the type of nonlinearity of proportional actions, 2) the inclusion of a linear function, and 3) the evaluation of nonlinearity variations for a given fuzzy controller. The issues are addressed below respectively.

Four simple types of nonlinear, or control, curves are identified in Fig. 8. These fundamental curves are defined within a positive region, $\hat{e} \in [0, 1]$ and $\hat{u}_P \in [0, 1]$. Types I and II exhibit *monotonic convex* and *concave* curves, respectively. Two other simple types are Types III and IV (Fig. 8(c), (d)), corresponding to *single-convex-plus-single-concave* curves. Only three types of curves, Types I, II, and III can be realized by the proposed controller. The need for fast rising of the proportional action in the middle range of $|\hat{e}|$, like Type IV curve in Fig. 8(d), may not be required for many applications. In general, if the nonlinear functions are more complex than those four types of curves, additional nonlinear tuning parameters are required. If a plant is lower order or with monotonic or essentially monotonic characteristics for a set-point control, a simple nonlinear curve may be sufficient for the controller without employing a complex nonlinear action. As a rule of thumb, in general nonlinear design, a controller having complex nonlinear-action behavior should have the flexibility to produce a simple action so as to adapt to those simple control situations.

Considering the issues of stability, controllability, and optimization of fuzzy systems [18], [36], we propose a conservative design strategy for fuzzy PID controllers—*A fuzzy PID controller should be able to perform a linear, or approximately linear, PID function such that the system performance is no worse than its conventional counterpart*. If the controller is able to include a perfect linear function as its property, we call it a *guaranteed-PID-performance* (GPP) system. We suggest that this GPP system should incorporate with an optimal solver for the specific performance index of interest, say, response error, stability, or robustness. Therefore, the system will produce the performance no lower than the corresponding linear PID system. This conservative design strategy is particularly important when we know that stability is guaranteed for a linear PID. In this case, we know immediately that the GPP fuzzy system will offer a safe performance bound with respect to the stability criterion. The performance analysis of a linear counterpart will provide a useful reference for the GPP fuzzy system design. In order to evaluate the confidence in using a GPP bound, we propose a *linearity approximation index* (LAI)

$$LAI = 1 - \frac{\max |\hat{u}_P(\hat{e}) - \tilde{u}_P(\hat{e})|}{\max |\hat{u}_P(\hat{e})|} \quad (20)$$

where \tilde{u}_P is a linear function from using a least square method of data \hat{u}_P . This function is imposed to pass through the origin point to satisfy Property B). Since the Euclidean distance error norm does not sensibly represent nonlinearity, the maximum-distance error norm is used. This index, representing the most linearity approximations which can be produced by the controller, is normalized within a range of $[0, 1]$. The larger the value of LAI, the higher degree of linearity approximation included by the fuzzy controller. The index provides a relatively quantitative measure of confidence in using a GPP bound for a fuzzy PID controller.

As shown later in the numerical studies, good performance of fuzzy PID controllers is attributed to their associated nonlinearities. The greater the nonlinearity variations, the greater the possibility of a high-performance controller. In order to evaluate a fuzzy PID controller according to its nonlinearity freedom, we propose a *nonlinearity variation index* (NVI), $NVI(N_v, N_p)$, where N_v and N_p are the total number of input variables associated with the fuzzy control action and the total number of nonlinear tuning parameters to tune the control action, respectively. The present controller has $N_v = 1$ and $N_p = 2$. NVI is defined as a process-independent measure and should be normalized within the range $[0, 1]$ for a consistent comparison between different controllers. For the present controller, we propose the following definition for $NVI(1, 2)$:

$$NVI(1, 2) = \frac{A_a(\theta_0, \theta_1)}{(\pi/2)^2} \quad (21)$$

where A_a is the *admissible area* for θ_0 and θ_1 of the present controller, and θ_0 and θ_1 are the angles in radians corresponding to NS_0 and NS_1 , respectively. Any point beyond this area cannot be realized by the present controller. For a linear PID (a unity line in Fig. 6), θ_0 and θ_1 are constants. This results in a point area only, and it gives $NVI(1, 0) = 0$. If $NVI(1, 2) = 1$, which is the maximum value for the index, it means that both θ_0 and θ_1 can be varied independently within $(0, \pi/2)$. For the present controller, θ_0 and θ_1 are not totally independent. From Property M), we can suppose θ_0 has a range of $[0, \pi/2)$, and then the ranges of θ_1 can be found from (18)

$$\left[\tan^{-1}\left(\frac{2z_0(2z_0+4)}{3(1-z_0)}\right), \tan^{-1}\left(\frac{4}{NS_0}\right) \right], \quad (NS_0 \neq 0), \quad x_1 \leq x_2$$

$$\left[\tan^{-1}\left(\frac{z_0(3z_0+4)}{3}\right), \tan^{-1}\left(\frac{2z_0(2z_0+4)}{3(1-z_0)}\right) \right], \quad (z_0 \neq 1), \quad x_1 > x_2. \quad (22)$$

Based on (22), we obtain the admissible area of a nonlinearity diagram for θ_1 and θ_2 (Fig. 9), which consists of Area A (gray area) from the nonoverlapping case, and Area B (hatched area) from overlapping case. Equation (19) then becomes

$$\begin{aligned} \theta_0 = 0, \quad \theta_1 \text{'s range} &= [0.37\pi, \pi/2), \quad \text{when } x_1 = 1 \\ \theta_0 = \pi/2, \quad \theta_1 = 0, & \quad \text{when } x_1 \rightarrow 0. \end{aligned} \quad (23)$$

The admissible area is calculated based on the two enclosure curves in (22)

$$\begin{aligned} NVI(1, 2) &= \frac{1}{(\pi/2)^2} \int_0^{\pi/2} \left\{ \tan^{-1}\left(\frac{4}{NS_0}\right) \right. \\ &\quad \left. - \tan^{-1}\left(\frac{z_0(3z_0+4)}{3}\right) \right\} d\theta_0 \\ &= \frac{0.0916\pi^2}{0.25\pi^2} = 0.366. \end{aligned} \quad (24)$$

Based on the admissible area of the nonlinearity diagram in Fig. 9, we now can find a point within the area which gives the best approximation to a linear PID controller. This point can be found mathematically using the least square method,

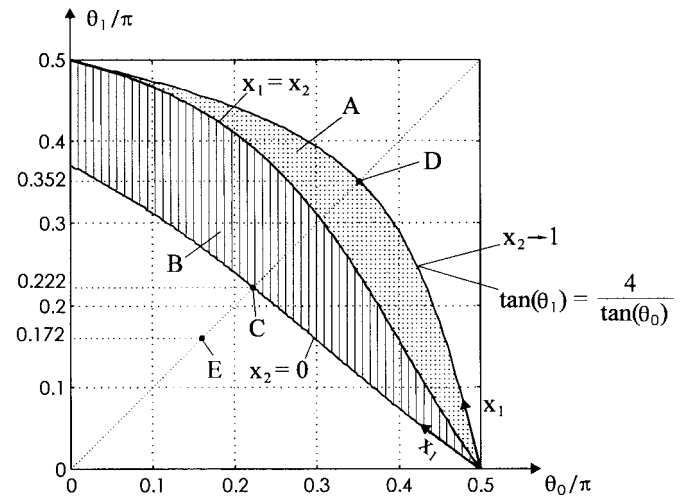


Fig. 9. Admissible area of nonlinearity diagram for θ_0 and θ_1 . A: gray area for nonoverlapping case. B: hatched area for overlapping case. C: point for approximation of a linear PID, corresponding to Curve C in Fig. 6. D: point corresponding to Curve D in Fig. 6. E: point calculated from (25).

but it involves a complex derivation. As an approximation, we suppose this point should satisfy the conditions

$$NS_0 = NS_1 = \frac{\max(|\hat{u}_P|)}{\max(|\hat{e}|)}. \quad (25)$$

This means that this point gives identical values for θ_0 and θ_1 . The identical values are not equal to a unity due to the partial normalization of \hat{u}_P (See Property C). The solution of (25) shows this point, Point E in Fig. 9, where $\theta_0 = \theta_1 = 0.172\pi$ (Note that for a full normalization of \hat{u}_P , $NS_0 = NS_1 = 1$, and $\theta_0 = \theta_1 = 0.25\pi$). This point (E) is outside the admissible area for θ_1 and θ_2 . Consequently, point C, which is closest to the E, is chosen as the best approximation point to a linear function. In Fig. 6, curve C, corresponding to point C when $x_1 = 0.466$ and $x_2 = 0$, illustrates this linear approximation. The linear regression line goes through the extreme point of $\hat{u}_P(\hat{e} = 1) = 2/3$. Thus the linear approximation index for the present controller is

$$LAI = 1 - \left(\max|\hat{u}_P - \frac{2}{3}\hat{e}| \right) / \left(\frac{2}{3} \right) = 0.9628. \quad (26)$$

This indicates that a good approximation of a linear relationship is included in the present fuzzy PID controller.

Three important observations can be obtained from this nonlinearity investigation. First, for any point within the admissible area, the further away from point C, the greater nonlinearity the “ \hat{u}_P versus \hat{e} ” curve represents. Therefore, the nonoverlapping case generally produces higher nonlinearity than the overlapping case. Second, four regions, Regions I, II, III, and IV, are approximately divided by point E (Fig. 10). Each region maps to the same number of curve type (say, Region I maps to Type I curve) in Fig. 8. Because there is no admissible area located in the Region IV, Type IV curve is unavailable from the present controller. Third, the tuning mechanism for the nonlinear tuning parameters is clearly described by the contour plot with respect to x_1 and x_2 as shown in Fig. 10. The incremental value for contour curves is

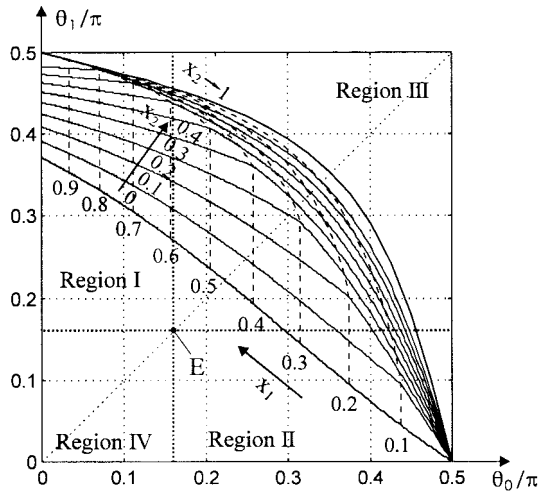


Fig. 10. Four regions for four types of simple nonlinear curves, and contour plot with respect to x_1 and x_2 in admissible area of nonlinearity diagram for θ_0 and θ_1 . $\Delta x = 0.1$. Dashed curves for x_1 and solid curves for x_2 .

$\Delta x_j = 0.1$ ($j = 1, 2$). Given x_1 and x_2 , the nonlinearity of the corresponding point is decided by the region number. The associated region number maps the type of nonlinear curve directly.

For a simple understanding of the tuning action with respect to the nonlinear tuning parameters, an example is given for the case when $x_1 = x_2 = x$, which corresponds to a touching case of the adjacent membership functions. The system, now to be a single-nonlinear-tuning-parameter controller, results in a single admissible line in the nonlinearity diagram (see the boundary between the overlapping and nonoverlapping in Fig. 9). Fig. 11 shows the nonlinear tuning for this system. When the tuning parameter x is increased, the associated nonlinear curve change from Type II to Type III, and finally to Type I. The best linear situation is when $x = 0.316$ [Fig. 11(b)]. The slope of the control curve corresponds to the normalized sensitivity. While this slope is fixed for a linear controller, it will change with error for a fuzzy PID controller. The desired property for this control curve is usually considered when \hat{e} is close to zero. A low value of NS_0 is preferred for a low degree of sensitivity to suppress the broadband noise from measurement around the set-point. On the other hand, a high degree of sensitivity is suggested in [7] and [9] for a fine tuning around this point by arranging denser membership functions around the zero-error point. In our case, this can be realized by allocating the small value of x to the consequent membership functions.

For a nonlinearity comparison study of different designs of a three-rule fuzzy PID controller, an alternative controller is developed in the Appendix. This study aims to display an analytical method for exploring the potentials and limitations of the fuzzy systems as a nonlinear approximator. The initial difference between the proposed controller and the alternative controller results from the membership functions of \hat{u}_P . The alternative controller has symmetric membership functions of the consequent fuzzy sets (Fig. 22 in the Appendix). Then, a fully normalized range of \hat{u}_P is offered to the alternative controller ($\max(|\hat{u}_P|) = 1$), while the proposed controller

has only partially normalized range as shown in Property C) ($\max(|\hat{u}_P|) \leq 1$).

The nonlinearity diagrams of admissible areas between two controllers are significantly different. The admissible area of the alternative controller (Fig. 23) is fully covered by the admissible area of the proposed controller (Fig. 9). This means that any nonlinear function produced by the alternative controller can be realized by the proposed controller, but not *vice versa*. Therefore, it is reasonable to consider that the proposed controller shows better design for its greater degree of nonlinearity variation. Table IV shows the nonlinearity comparison between the two controllers. It is interesting to find out that, while a minor change is made to the membership functions of fuzzy controllers, their corresponding nonlinearity variations may change significantly.

The investigation of the controller in regard to its associated NVI is of great help to demonstrate the potential and limitation of the controller. For example, a diagram of admissible areas/lines/points can explain the reason why a fuzzy PID controller may fail to provide better performance than a conventional PID controller. Suppose that a specific process needs a perfect linear function for the high-performance control. If those admissible areas/lines/points produced by a fuzzy controller do not cover the point for a perfect linear function, the fuzzy controller, of course, presents poorer performance than a linear PID controller. Using the NVI as a process-independent measure, designers are able to improve the design in the selection of the fuzzy rules, membership functions, inference schemes, etc.

IX. GENETIC-BASED OPTIMAL DESIGN

Controller design decisions should be made based on the specific performance criteria. Suppose J_T is the overall performance index of the system, which is in a form for a fuzzy PID controller

$$J_T = f(\hat{K}_P, \hat{K}_I, \hat{K}_D, \text{MF's}, \text{SF's}) \quad (27)$$

where MF's are the membership functions for the fuzzy rules, and SF's are scaling factors. Usually, there is a nonlinear relationship between the overall performance index and the design parameters. In addition, J_T may have multimodal characteristics, and the standard gradient-descent optimization may trap into a local optimization. In this work, we apply genetic algorithms (GA's) for high-performance controller design. By mimicking the principles of natural selection, GA's are able to evolve a solution to real-world problems. Unlike the gradient algorithms, GA's are not mathematically guided solvers. The advantage of the GA's is its global optimization solution even for nonlinear, high-dimensional, multimodal, and discontinuous problems [10]. Although there are many variations of off-line and on-line approaches [21], [22], we focus on the simple genetic algorithm developed in [10]. In this study, the GA parameters are given by: number of generations = 100; population size = 100; crossover factor (P_c) = 0.9; mutation factor (P_m) = 0.05; and binary bits of parameters = 7. The generalized optimization problem for the

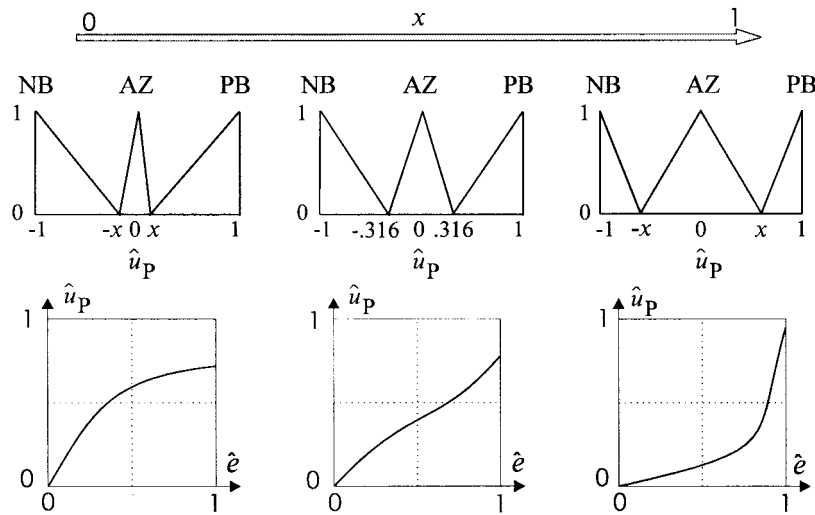


Fig. 11. Nonlinear tuning with respect to x ($=x_1 = x_2$). (a) Type II (small x). (b) Type III (small $x = 0.316$). (c) Type I (big x).

TABLE IV
DIFFERENCES AND NONLINEARITY COMPARISON BETWEEN THE PROPOSED CONTROLLER AND THE ALTERNATIVE CONTROLLER

	Proposed Controller	Alternative Controller
Ranges of MFs for \hat{u}_p	$[-1, 1]$	$[-(1+x_2), (1+x_2)]$
$\max \hat{u}_p $	$(2+x_2)/3$	1
LAI	0.963	0.959
NVI	0.366	0.0908
Types of nonlinear curves	I, II, III	I, II, III

controller is described as

$$\begin{aligned} & \text{maximize } F(\hat{K}_P, \hat{K}_I, \hat{K}_D, s_u, x_1, x_2) = 1/(1 + J_T) \\ & \text{subject to (6)} \\ & G(\hat{K}_P, \hat{K}_I, \hat{K}_D, s_u, x_1, x_2) \leq 0 \end{aligned} \quad (28)$$

where F is a fitness function and G is a constraint function from the performance requirement (say, the restraint for the normalized sensitivity). The objective function using fitness value produces uniformity from its normalized range $[0, 1]$. It relates to the overall performance index from a sum of the weighted individual performance indexes

$$\begin{aligned} J_T(\hat{K}_P, \hat{K}_I, \hat{K}_D, s_u, x_1, x_2) \\ = \sum_{i=1}^m w_i J_i(\hat{K}_P, \hat{K}_I, \hat{K}_D, s_u, x_1, x_2) \end{aligned} \quad (29)$$

where w_i is a weight associated with the i th individual performance index J_i . Weighting is used in the case that indexes have large difference in their magnitudes; and it can also emphasize some specific performance indexes over others. In order to be compatible with the normalization technique, each individual performance index should be dimensionless and represented in terms of error for consistency. As a result, the smaller J_T , the better the performance. This shows that a high value of F corresponds to good performance.

Performance assessment based on response error signals is conducted but it is difficult to optimal control due to the

conflicting performance requirements between static accuracy (steady-state error) and dynamic responsiveness (speed of response). Most studies have applied a single-error criterion for representing overall performance [17], [30], [42]. However, we find that a single performance index may lead to poor design with respect to other performance indexes (see Example 6 in the numerical studies). In this work, three individual indexes ($m = 3$) are applied

$$J_T = w_1 \frac{\text{ISE}}{\max(e(n))} + w_2 \text{POS} + w_3 \frac{T_s}{T} \quad (30)$$

where ISE is integral of the square of the error over the total simulation time T ; T_s is settling time, and the POS is the percent overshoot [8]. For a unit step response, we assume that $\max(e(n)) = 1$.

X. NUMERICAL STUDIES

In this section, numerical studies are conducted to examine the performance of the proposed fuzzy PID controllers. Comparisons are made with the conventional linear PID, and heuristically rule-tuned PID controllers. For a fair comparison, the conventional linear PID are also designed using the same optimal criteria for the testing. The present genetic-based optimization usually does not give the same results for each calculation. (The fitness results are close but may have distinct design parameters.) This phenomenon implies two indications: the method is a near-optimization approach, and the sets of

TABLE V
PERFORMANCE COMPARISON IN EXAMPLE 1

	Optimal Fuzzy PID	Optimal PID
$\hat{K}_p, \hat{K}_i, \hat{K}_D$	1.0, 0.394, 0.0	1.0 1.0, 0.0
x_1, x_2, s_u	0.0079, 0.630, 7.32	-, -, 10.0
T_r (sec.)	0.16	0.20
T_s (sec.)	0.20	0.36
POS (%)	0.0	0.39
ISE	0.0653	0.0590
ITSE	0.0023	0.0023
F	0.858	0.805

the distinct searching parameters represent the multimodal property in the optimization problem.

The proposed fuzzy PID system, like other fuzzy control systems, assumes no mathematical model of a control process. Without knowledge of a plant, the system searches for the optimal tuning parameters automatically (this is also true for the proposed optimal linear PID controller). As a preliminary study, the validity of the proposed system is tested only on a single-input and single-output process for set-point control tasks. Two basic low-order processes are initially investigated, followed by a fifth-order process. For each plant, all initial conditions are set to be zero and saturation is included at the plant input. Six examples are studied using Matlab’s Fuzzy Logic Toolbox [16]. The Runge–Kutta third-order method is used for all simulations. A unit step response is studied to simulate set-point control. The sampling time is set at 0.02 s unless otherwise specified. In calculation of the overall performance (29), an even weighting value $w_i = 1$ is given for each individual index from Examples 1 to 5. The different weighting is tested in Example 6. In order to better interpret the mathematical models of the processes, some examples are related to the physical systems in common industrial applications. After the implementation of the controller system, a simple analysis is made based on the conventional control theory to verify the design.

Example 1. A First-Order Process Without Time Delay: Many industrial processes, such as temperature, pressure, pH value, and fluid-level controls, can be approximated by a first-order model. A three-term model of a first-order process is generally given by

$$G(s) = \frac{K}{t_c s + 1} e^{-t_d s} \tag{31}$$

where t_c , t_d , and K are time constant, time delay, and the steady-state gain of the plant, respectively. A temperature control process without time delay is assumed for this example [23]. For a heater plant, a nonnegative range has defined for u .

$$t_c = 1 \quad t_d = 0 \quad K = 1 \quad u_{\min} = 0 \quad u_{\max} = 10.$$

The step responses of the two optimal controllers are shown in Fig. 12. The three gains are automatically determined by the genetic search for two optimal controllers. The conclusion obtained from this example for both controllers is that this process does not require a derivative action with respect to

the present performance requirement (30), that is, $\hat{K}_D = 0$. Note that a fuzzy PD controller was used for the same process in [23]. The selection of PI-type controllers from the present system can be understood by a simple analysis in examining the transfer function G_C of the closed-loop process (without the controller) [8]

$$G_c(s) = G(s)/[1 + G(s)] = 1/[s + 2].$$

Two characteristics of the process explain the optimal results. First, the steady-state error of the process is nonzero ($e_{ss} = 0.5$), which suggests a requirement for an integral law in the process. The integral term is sometimes called a *reset* because it is associated with setting a steady offset in the control input. Here, an integral action is a necessary condition for a zero steady-state error of the process. The constant control input to a heater is calculated by this law for maintaining a unit temperature to the plant. Second, G_C remains to be a first-order process which has no oscillation. It is known that a derivative law has a damping effect on oscillation but results in a sluggish response. Since the present closed-loop temperature plant does not exhibit oscillatory behavior, the derivative action is unnecessary for the response error criteria.

The results of the performance indexes for each controller are listed in Table V, where the rise time (T_r), and the integral of time multiplied by the squared error (ITSE) [8] are also presented for a broader comparison of individual performance indexes. It is clear that the fuzzy controller gives better overall performance. However, if the ISE is used for single-index optimization, a different conclusion—that the linear PID produces better performance than the fuzzy PID controller—is reached. A careful selection of performance indexes is important for optimal design. In Example 6, we will demonstrate more results for the different index selections.

The two controllers show a small difference ($= 6.58\%$) in terms of the fitness function (Table V). However, there is a significant difference in the response curves around the controlling Zone A as illustrated in Fig. 12. *While the conventional PI controller reaches the set-point smoothly, a fuzzy controller is able to produce a sharp-curve-like response.* This characteristic is attributed to the nonlinearities of fuzzy systems. While Curve A in Fig. 6 shows a Type-II nonlinear proportional action, Fig. 13 clearly illustrates the nonlinear tuning actions for two gains of the system in the error domain. Both gains are symmetric with respect to \hat{e} [Fig. 13(a) and

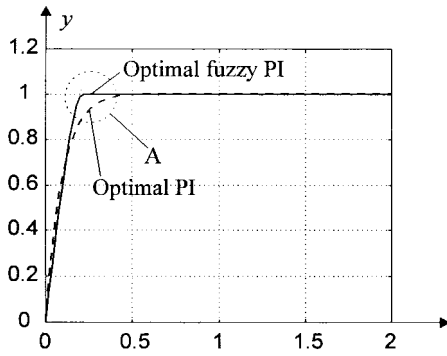


Fig. 12. Step responses of optimal PID and optimal fuzzy PID in Example 1.

(c)]. The plot of Fig. 13(a) is obtained from the closed-form solution, but the plots in Fig. 13(b) and (c) are obtained from numerical simulations. While the conventional PID gains are constant, the fuzzy controller exhibits self-tuning capability with respect to variations in \hat{e} and/or $\sum \hat{e}$. When the temperature of the plant approaches the set point, the equivalent gains of \hat{K}_P and \hat{K}_I are increased to realize a sharp-curve-like action (but this action is sensitive to the noise around the set point). This is why a fuzzy controller shows a better performance than a linear controller. Heuristic knowledge can be extracted from the optimal tuning actions from the gain plots in Fig. 13 for manual tuning. This operation is usually based on an error domain [Fig. 13(a) and (c)], rather than on a sum-of-error domain [Fig. 13(b)]. Therefore, we will show the gain plots only with respect to error in the later examples.

Example 2. A First-Order Process with a Time Delay: The time delay occurs when a sensor (e.g., a thermocouple) and an actuator (e.g., a heater) are installed with a physical separation. The effect of the time delay in the first-order process in Example 1 is examined next. The process parameters in (31) are chosen as

$$t_c = 1 \quad t_d = 0.2 \quad K = 1 \quad u_{\min} = 0, u_{\max} = 10.$$

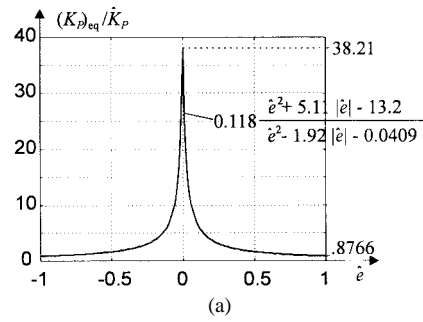
A comparison is made with PI/PID controllers tuned using the Ziegler–Nichols (Z–N) approach [2]. The Z–N gains are calculated from the three terms of the process [2]

$$\text{Z–N tuned PI: } K_P = 4.5, \quad K_I = 7.5.$$

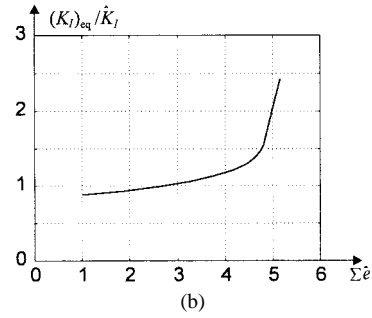
$$\text{Z–N tuned PID: } K_P = 6, \quad K_I = 15, \quad K_D = 0.6.$$

The step responses of four controllers are shown in Fig. 14. As in Example 1, the GA optimization results in PI-type systems again for both linear and fuzzy controllers. Both optimal controllers produce significant improvements over the Z–N PI/PID controllers. The difference of the fitness F between optimal PI and optimal fuzzy controllers becomes larger (= 14.0%, Table VI) than that observed in Example 1, which is due to the nonlinearity introduced by the time delay. While the linear PID controller has no self-tuning function for process nonlinearity, the present fuzzy controller has the capacity to self adjust. These two examples demonstrate that *fuzzy controllers may present a significant improvement in control performance for a time-delayed process.*

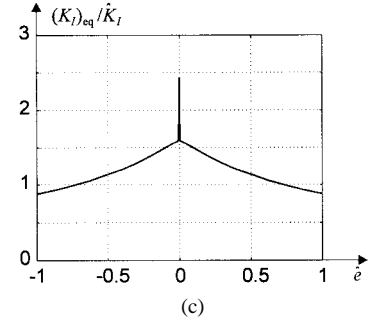
Fig. 15 shows the nonlinearity variations of the two gains in this delayed first-order process. The main difference with



(a)



(b)



(c)

Fig. 13. Gain plots for the optimal fuzzy PI in Example 1. (a) “ $(K_P)_{eq}/\hat{K}_P$ versus \hat{e} ” plot from a closed-form solution. (b) “ $(K_I)_{eq}/\hat{K}_I$ versus $\sum \hat{e}$ ” plot from a numerical simulation. (c) “ $(K_I)_{eq}/\hat{K}_I$ versus \hat{e} ” plot from a numerical simulation.

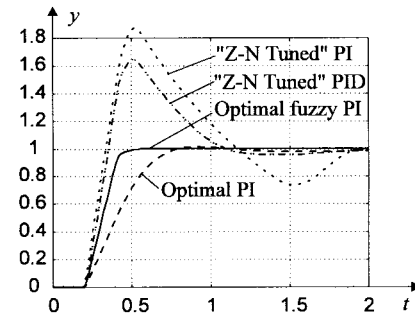


Fig. 14. Step responses of “Z–N tuned” PI/PID, optimal PI, and optimal fuzzy PI in Example 2.

Example 1 can be observed from the proportional actions. When a time delay is added, a Type I nonlinear curve is selected (Curve B in Fig. 6), while changing the tuning actions of two gains accordingly (Fig. 15). The overall magnitudes of both gains are decreased compared with those in Example 1 (Fig. 13) since the sluggish characteristics have been added to the process. It is also interesting to see that the highest magnitudes for both gains move to the extreme points of the error.

TABLE VI
PERFORMANCE COMPARISON IN EXAMPLE 2

	Optimal Fuzzy PID	Optimal PID
$\hat{K}_P, \hat{K}_I, \hat{K}_D$	1.0, 0.961, 0.0	1.0, 0.874, 0.0
x_1, x_2, s_u	0.874, 0.945, 4.57	-, -, 2.52
T_r (sec.)	0.16	0.38
T_s (sec.)	0.46	0.74
POS (%)	0.51	1.62
ISE	0.286	0.345
ITSE	0.0394	0.0629
F	0.658	0.577

TABLE VII
PERFORMANCE COMPARISON IN EXAMPLE 3

	Optimal Fuzzy PID	Optimal PID
$\hat{K}_P, \hat{K}_I, \hat{K}_D$	1.0, 0.0, 0.874	1.0, 0.0, 0.449
x_1, x_2, s_u	0.102, 0.260, 25	-, -, 25
T_r (sec.)	0.42	0.48
T_s (sec.)	0.64	0.72
POS (%)	1.83	1.98
ISE	0.249	0.234
ITSE	0.0364	0.0337
F	0.630	0.620

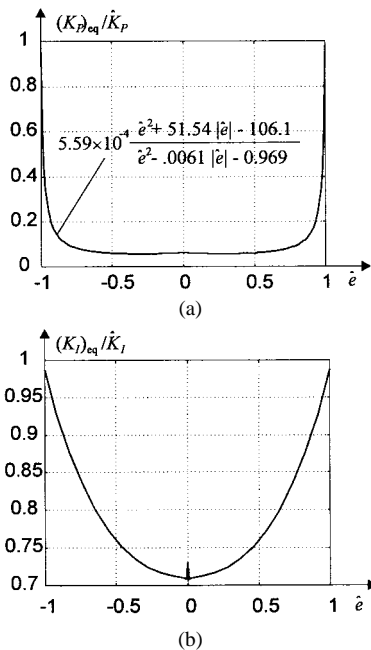


Fig. 15. Gain plots for the optimal fuzzy PI in Example 2. (a) “ $(K_P)_{eq}/\hat{K}_P$ versus \hat{e} ” plot from a closed-form solution. (b) “ $(K_I)_{eq}/\hat{K}_I$ versus \hat{e} ” plot from a numerical simulation.

Example 3. A Second-Order Process Having a Zero Steady-State Closed-Loop Error: This example follows the work in [19] and [2, Example 11.2]. The plant is a second-order process

$$G(s) = 1/[s(s + 1)]$$

such as position control of an ac motor [8]. The saturation range is given as (see [19, fig. 8])

$$u_{min} = -5 \quad u_{max} = 25.$$

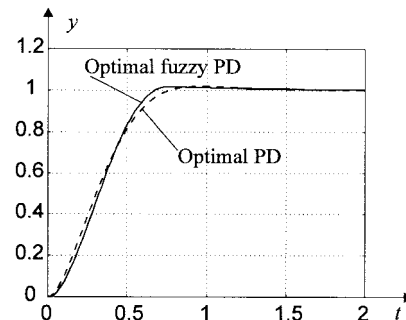


Fig. 16. Step responses of optimal PD and optimal fuzzy PD in Example 3.

Based on the optimization, both the linear and fuzzy controllers arrive at the same results regarding integral action (i.e., $\hat{K}_I = 0$). This differs from the results of [19], where a fuzzy PI controller was used. Fig. 16 shows the step responses of both optimal linear PD and optimal fuzzy PD controllers. A detailed comparison of performance is listed in Table VII. The transfer function reveals the oscillation property inherent in the closed-loop process

$$G_c(s) = 1/(s^2 + s + 1).$$

The closed-loop model is equivalent to a damped vibration system with a natural frequency of $\omega_n = 1$ rad/s with the associated damping ratio of $\xi = 0.5$. A derivative term is required to suppress the vibrations of the closed-loop process. The steady-state closed-loop error of this process is zero ($e_{ss} = 0$). The self-regulating property of the system suggests that there is no need to employ integral action for the process. The physical interpretation is that the motor is controlled to move by a unity angle and then to stop. When a steady state is reached,

TABLE VIII
PERFORMANCE COMPARISON IN EXAMPLE 4

	C1	C2	C3
u_{max}	10	5	5
u_{min}	0	0	0
\hat{K}_P, s_u x_1, x_2	0.787, 8.98 0.323, 0.913	same as C1's	0.787, 4.65 0.102, 0.937
T_r (sec.)	0.76	0.74	0.88
T_s (sec.)	1.14	2.34	1.34
POS (%)	1.72	6.22	1.07
ISE	0.310	0.348	0.387
ITSE	0.0658	0.0799	0.0991
F	0.620	0.501	0.577

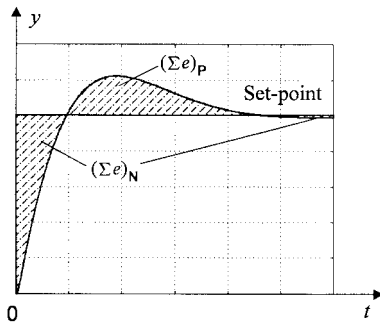


Fig. 17. Step Response of a controller including an integral law in Example 3.

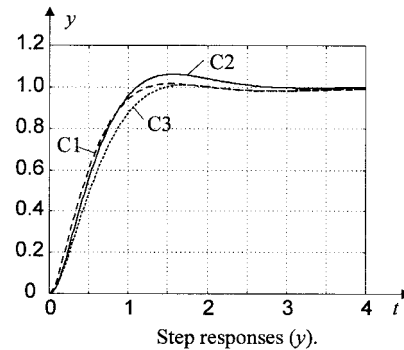
the process requires no control input, that is, $u_{ss} = 0$. If an integral law is applied, the response will be forced to undergo an overshoot before reaching the steady state in order to compensate for the negatively accumulated error (Fig. 17). Therefore, any integral action will decrease the performance by including overshooting and possible oscillation from unbalanced compensation. From this simple analysis, the heuristic design guideline required is that a PD-type controller will produce an optimal performance [in the sense of (29)] for a closed-loop zero steady-state error process (or the "Type 1 or higher systems" [8] with the unity negative feedback for a step input).

Example 4. A Second-Order Process with Overdamping: Many temperature control plants can also be modeled by a second-order process with overdamping. The fourth example is a process with a transfer function of [23]

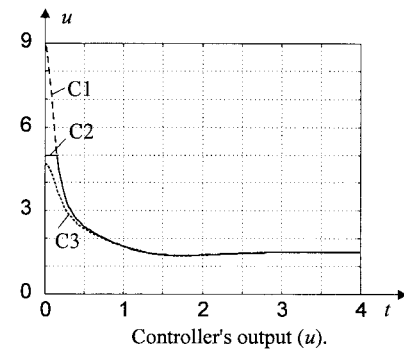
$$G(s) = 2/(s^2 + 4s + 3).$$

In this example, we examine the saturation effect on the process performance. Three fuzzy controllers, namely, C1, C2, and C3, are investigated. While the lower bounds of saturation are always kept the same, $u_{min} = 0$, for the three controllers, the upper bounds are given different values. C1 has $u_{max} = 10$, and C2 and C3 have $u_{max} = 5$, for the heater input. Both C1 and C3 are independently designed to take account of the different associated saturation ranges (Table VIII). However, the response of C2 is evaluated using the same design parameters as C1, but has the same saturation range as C3.

A fuzzy PI controller is initially investigated. Four tuning parameters are selected according to Table III, and remaining



(a)



(b)

Fig. 18. Plots of C1, C2, and C3 controllers (Fuzzy PI) in Example 4. (a) Step responses (y). (b) Controller's output (u).

two parameters are $\hat{K}_P = 1$ and $\hat{K}_D = 0$. Comparing the fitness value F of each controller in Table VIII, as well as the step responses in Fig. 18(a), we find C2 has the poorest performance although it has the same design parameters as C1. The deteriorated performance is caused by an integral windup [2] that keeps integrating even though the control input has been saturated. Sometimes, an antiwindup gain with a feedback to the control input or additional rules are added to solve this problem [19]. Other schemes using fuzzy systems are found in [13]. In this process, the controller output curve of C3 in Fig. 18(b) is dropped automatically at the beginning of the process for preventing the windup. The simulation results suggest that the genetic-based optimization methods perform the antiwindup function without adding extra design parameters for antiwindup. This is understandable that

TABLE IX
PERFORMANCE COMPARISON IN EXAMPLE 5

	Optimal Fuzzy PID	Optimal PID
$\hat{K}_P, \hat{K}_I, \hat{K}_D$	0.929, 0.110, 1.0	0.906, 0.173, 0.709
x_1, x_2, s_u	0.0315, 0.606, 9.53	-, -, 9.53
T_r (sec.)	0.44	0.78
T_s (sec.)	0.68	1.18
POS (%)	0.841	1.58
ISE	0.314	0.358
ITSE	0.0561	0.0897
F	0.602	0.505

TABLE X

	Z-N PID [42]	Å-H PID [42]	Z-A PID [42]	Optimal Fuzzy PID
K_P, K_I, K_D	1.61, 0.358, 1.81	1.88, 0.273, 3.25	1.62, 0.307, 1.89	0.709, .0787, .724
x_1, x_2, s_u	-	-	-	.740, .961, 9.37
T_r (sec.)	4.2	3.5	4.6	2.5
T_s (sec.)	20.1	22.8	19.2	6.5
POS (%)	18.0	14.6	8.5	2.26
ISE	-	-	-	2.25
ITSE	-	-	-	2.21
F	-	-	-	0.287

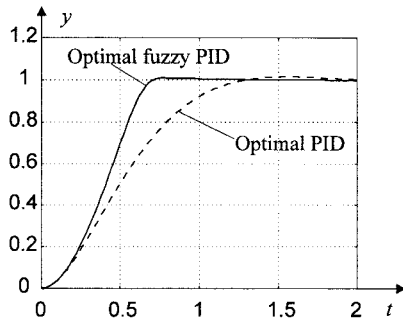


Fig. 19. Step responses of optimal PID and optimal fuzzy PID controllers in Example 5.

if we consider the method, which is based on a principle of performance selection, removes the candidate solution that is deteriorated by the windup. Further investigation is also made using a fuzzy PID controller for the same process. The response performance is improved due to the inclusion of derivative actions (The closed-loop process has a natural frequency $\omega_n = \sqrt{5}$ rad/s with the associated damping ratio of $\xi = 0.894$). Again, the simulation results confirm the finding of antiwindup functions of the proposed fuzzy controllers.

Example 5, A Second-Order Process with a Small Damping Ratio: A second-order process with a small damping ratio is examined. The general form of the process is

$$G(s) = \frac{\omega_n^2}{s^2 + 2\xi\omega_n s + \omega_n^2}$$

where ω_n and ξ are the natural frequency and damping ratio of the process, respectively. This example is similar to a mass-spring-damper system and we take the following parameters:

$$\omega_n = 1 \quad \xi = 0.01 \quad u_{\min} = -10 \quad u_{\max} = 10.$$

This process requires all three gains, \hat{K}_P , \hat{K}_I , and \hat{K}_D , due to the oscillation and nonzero steady-state error in the closed-loop process. The optimal fuzzy PID controller is compared with the optimal linear PID controller (Fig. 19). The detailed comparison of performance is listed in Table IX. Due to the small damping ratio, the process puts more weight on the derivative action than on the integral action in this example. The difference between the optimal PID and optimal fuzzy PID controllers is significant (= 19.2%) although the process is linear. In the interest of gaining heuristic tuning knowledge for tuning this process, the plots of three gains are presented in Fig. 20. Generally, all three gains reach their maxima when the error is small.

Example 6. A Fifth-Order Process: In this example, a fifth-order process is studied. The transfer function of the process is [42]

$$G(s) = 1/(s + 1)^5.$$

Since this model did not give the saturation ranges, we initially make a calculation on $u_{\min} = -10$ and $u_{\max} = 10$. If the simulation results show $s_u = 10$, the saturation range can be increased for a better performance. The sampling time is chosen as 0.5 s. The purpose of this study is to show the applicability of the proposed fuzzy PID system to a high-order process. Table X presents the detailed comparison results of optimal fuzzy PID with the Ziegler–Nichols, Åström–Hägglund (Å–H) [1], and Zhuang–Atherton (Z–A) [42] rule-tuned PID systems. Significant improvement in performance is obtained compared with other approaches (Table X). It should be noted that all other rule-tuned PID controllers [1], [2], [42] are implemented with less effort and by using simple calculations based on heuristic rules. However, the three times differences in the settling time as well as in the overshoot in this example suggest

TABLE XI
PERFORMANCE COMPARISON IN EXAMPLE 6

	Optimal PID		
	P1 (based on F)	P2 (based on F_1)	P3 (based on F_2)
$\hat{K}_P, \hat{K}_I, \hat{K}_D$	0.394, 0.0630, 0.992	0.213, 0.0394, 0.0630	0.906, 0.323, 0.575
s_u	4.17	8.90	0.551
T_r (sec.)	2.5	2.5	5.5
T_s (sec.)	16.5	25	9.5
POS (%)	4.55	13.2	0.923
ISE	3.08	2.96	4.36
ITSE	4.56	4.51	9.65
F	0.214	0.203	0.176
F_1	0.245	0.253	0.186
F_2	0.104	0.0805	0.117

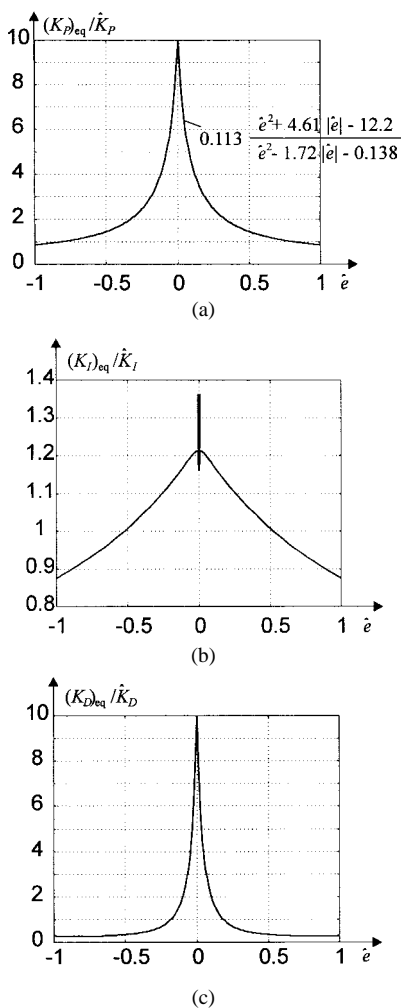


Fig. 20. Gain plots for the optimal fuzzy PID in Example 5. (a) “ $(K_P)_{eq}/\hat{K}_P$ versus \hat{e} ” plot from a closed-form solution. (b) “ $(K_I)_{eq}/\hat{K}_I$ versus $\sum \hat{e}$ ” plot from a numerical simulation. (c) “ $(K_D)_{eq}/\hat{K}_D$ versus \hat{e} ” plot from a numerical simulation.

a worthwhile application of an optimal fuzzy PID system, although an extra computing cost is added in the design.

Further investigation is made on the selection of the performance index and its associated weighting for the optimal linear

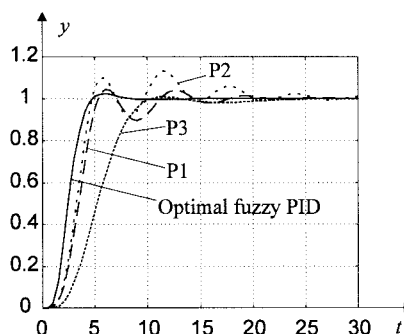


Fig. 21. Step responses of optimal PID (P1–P3) and optimal fuzzy PID-type controllers in Example 6.

PID systems. In addition to the original F , two different fitness functions, F_1 and F_2 , are also employed for the optimization

$$F_1 = \frac{1}{1 + \text{ISE}} \quad F_2 = \frac{1}{1 + \text{ISE} + \text{POS} + 10\frac{T_s}{T}}$$

Note that the F_1 , including a single-performance index, is in principle the same as used in [42], where they have used the ITSE as the single-performance index. The F_2 is adding a higher weighting value to the settling time for the original F . As we can see, a single-index performance using the error sum, like P2 curve in Fig. 21, may produce a large overshoot and a long settling time. A multiple-index performance, say, P1 and P3 curves, are preferred in applications.

Nonlinearity Comparison Among the Six Numerical Examples: Six numerical examples were investigated. Within those examples, the fuzzy PID controllers always present the best performance results. For a better comparison of the nonlinearity selected by the optimal method corresponding to each process, we list the related data in Table XII. Out of the four basic nonlinear curves, only Types I and II nonlinear curves, corresponding to the simplest, are selected from the optimization. None of the controller systems selects Type III. It is also interesting to know that all curves correspond to a nonoverlapping case ($x_1 < x_2$). All systems resort to a great degree of nonlinearity (LAI = 0.231 ~ 0.765) for high performance of the processes.

TABLE XII
NONLINEARITY COMPARISON AMONG THE SIX NUMERICAL EXAMPLES

Example	Plant	Fuzzy PID-type	Nonlinear curve type	LAI
1	First-order without time delay	PI	II	0.409
2	First-order with time delay	PI	I	0.254
3	Second-order with a zero pole	PD	II	0.765
4-C1	Second-order with overdamping	PI	I	0.479
4-C3		PI	I	0.655
5	Second-order with a small damping	PID	II	0.597
6	Fifth-order with the same poles	PID	I	0.231

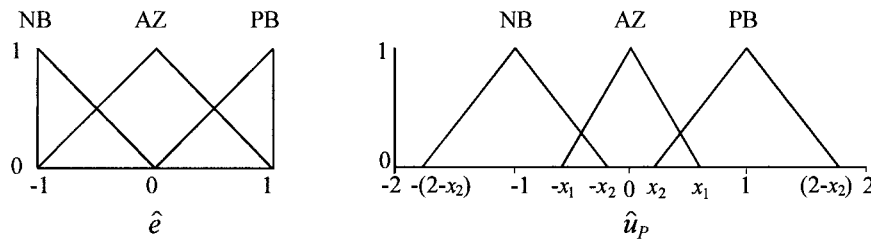


Fig. 22. Membership functions of an alternative three-rule fuzzy controller.

XI. SUMMARY

This paper describes a novel methodology to study fuzzy systems analytically. A closed-form solution to the fuzzy inference is pursued to bridge the fuzzy theory and classical/modern control theory. This investigation has clearly displayed that fuzzy control techniques are possible to present a general framework for linear/nonlinear controllers. We believe that the study of fuzzy controllers should be exploded in the light of nonlinear control principle and reinforced by integrating traditional and modern control theories.

One significant contribution of this work is the development of a simple fuzzy PID controller using a single input variable with three rules and at most six design parameters. Comparing with a linear PID controller, the proposed fuzzy system adds only two more parameters for nonlinear tuning. This structure simplifies the system design significantly from the generation of a control curve, rather than a control surface. The nonlinearity is explicitly defined for fuzzy proportional actions in the error domain. Important properties of the fuzzy PID system are derived for providing the guidelines of nonlinear designs. Moreover, the physical meaning of the nonlinear tuning parameters becomes clear for tuning actions from the admissible area of a nonlinearity diagram.

Another contribution of this work is the suggestion of two indexes for nonlinear controller design. The first is a LAI for a guaranteed-PID performance fuzzy system based on a conservative design strategy. This strategy suggests a fuzzy PID controller can replace conventional PID controller by augmenting the linear function. The proposed fuzzy system produces a close approximation of linearity. Therefore, the

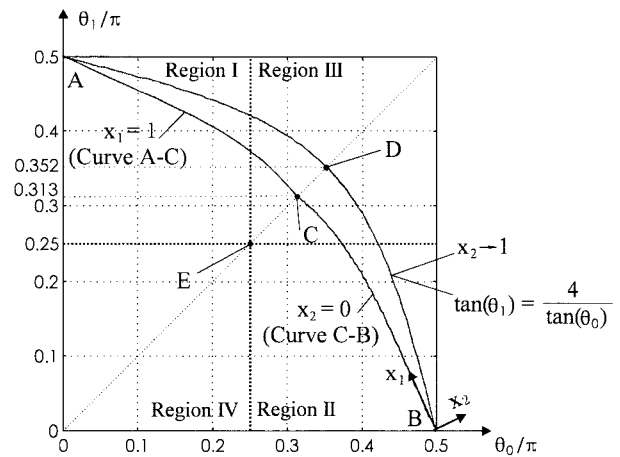


Fig. 23. Admissible area of nonlinearity diagram for θ_0 and θ_1 of the alternative controller. *C*: point for approximation of a linear PID, corresponding to $x_1 = 0$, and $x_2 = 1$. *E*: point calculated from (24).

performance analysis of linear PID systems will provide approximately a lower performance bound of the specific performance criteria (for example, the response error in this work) for the proposed fuzzy systems. The second index, NVI, is proposed for evaluating the degrees of freedom for producing nonlinearities in a fuzzy PID system. Using these indexes and nonlinearity diagram proposed in this work, the control designer can immediately interpret the controllers in regard to its nonlinearity abilities on the following aspects: 1) the classes of nonlinear curves possibly produced by the controllers; 2) the range of nonlinearity variation encompassed for each class of nonlinear curves; and 3) the capability to

$$NS_1 = \left. \frac{\partial \hat{u}_p}{\partial \hat{e}} \right|_{\hat{e}=1} = \begin{cases} 2 \frac{1-x_2}{1-x_2}, & x_1 \leq x_2 \\ \frac{1}{3} \left[\frac{x_1}{-3 + 15x_1 + 13x_2 - 12x_1x_2 + 6x_1^2 - 14x_2^2 - 4x_1^2x_2 + 4x_2^3} \right], & x_1 > x_2 \end{cases} \quad (A.8)$$

approximate a linear function. A comparative study from the viewpoint of nonlinear designs was made between the proposed system and an alternative system. This comparative study clearly demonstrates that an in-depth analytical approach is a useful tool for an efficient fuzzy controller design.

The present system can operate as both fuzzy PID (including an approximate linear PID function), or linear PID versions on an optimal basis. The work results in a standard implementation methodology for the design. These include normalizing error and three gains, using normalized fitness function from the multiple performance indexes, and considering actuator saturation ranges.

Numerical studies are reported on several processes having different response characteristics. For all six processes, comparisons of the control performance are made between conventional PID and the proposed fuzzy PID controllers. Genetic-based optimization solvers are used for fair comparisons. The proposed system always provides the best control performance. In comparison of the optimal linear PID controller with heuristic methods, the Ziegler–Nichols, Åström–Hägglund, and Zhuang–Atherton rule-tuned PID controllers were also tested for a fifth-order plant. Significant improvement of performance suggests it worthwhile to apply the proposed fuzzy controllers.

APPENDIX

AN ALTERNATIVE THREE-RULE FUZZY PID CONTROLLER

An alternative three-rule fuzzy PID controller is developed for a comparison with the proposed controller in Fig. 4. The membership functions of \hat{u}_P for the alternative controller are extended to a range of $[-1-x_2, 1+x_2]$, as shown in Fig. 22. The change, making the \hat{u}_P to be fully normalized, is for noninfluence to the s_u when x_2 is adjusted. The change also simplifies the closed-form derivation of fuzzy proportional actions.

Based on the same fuzzy reasoning method, the fuzzy proportional action of the alternative controller is also represented by two cases as below.

Case 1 (Nonoverlapping): $x_1 \leq x_2$

$$\hat{u}_p = \frac{\hat{e}(2-|\hat{e}|)(1-x_2)}{(2|\hat{e}|-\hat{e}^2)(1-x_2) + (1-\hat{e}^2)x_1}. \quad (A.1)$$

Case 2 (Overlapping): $x_1 > x_2$

Range A: $0 \leq |\hat{e}| \leq \hat{e}_d$

$$\hat{u}_p = \frac{\hat{e}}{3} \left[\frac{(y_2^2 - x_1^2)(3z_1^2 + \hat{e}^2) + 3y_2(2-|\hat{e}|) + 3}{(x_1 + y_2)(2|\hat{e}| - \hat{e}^2) + 2x_1z_3 + 2|\hat{e}|} \right]. \quad (A.2)$$

Range B: $\hat{e}_d < |\hat{e}| < 1 - \hat{e}_d$

$$\hat{u}_p = \frac{\hat{e}}{3|\hat{e}|} \left[\frac{(y_2^2 - x_1^2 - 2x_1 - y_2)\hat{e}_d^2 + 6|\hat{e}|y_2(2-|\hat{e}|)}{2x_1 + 4y_2|\hat{e}| - (x_1 + y_2)(\hat{e}_d^2 + 2\hat{e}^2)} \right]. \quad (A.3)$$

Range C: $1 - \hat{e}_d \leq |\hat{e}| \leq 1$

$$\hat{u}_p = \frac{\hat{e}}{3|\hat{e}|} \left[\frac{(y_2^2 - x_1^2)(3-3|\hat{e}| + \hat{e}^2)|\hat{e}| + 3y_2(4|\hat{e}| - 1) + 3|\hat{e}|}{(x_1 + y_2)(2|\hat{e}| - \hat{e}^2) + 2y_2(2|\hat{e}| - 1) + 2|\hat{e}|} \right] \quad (A.4)$$

where some intermediate variables are defined as

$$z_1 = 1 - |\hat{e}| \quad z_3 = 1 - 2|\hat{e}| \quad y_2 = 1 - x_2 \quad (A.5)$$

and \hat{e}_d , a *division point*, is calculated by

$$\hat{e}_d = \frac{x_1 - x_2}{1 + x_1 - x_2}. \quad (A.6)$$

The normalized sensitivities at two points are

$$NS_0 = \left. \frac{\partial \hat{u}_p}{\partial \hat{e}} \right|_{\hat{e}=0} = \begin{cases} 2 \frac{x_1}{1-x_2}, & x_1 \leq x_2 \\ \frac{4-4x_2-x_1^2+x_2^2}{2x_1}, & x_1 > x_2 \end{cases} \quad (A.7)$$

The differences of the properties of this controller from the proposed controllers are given in (A.8) at the top of the page. A fully normalized proportional control output is obtained; that is, $\max(|\hat{u}_P|) = 1$. Fig. 23 shows the admissible area for θ_0 and θ_1 . While the nonoverlapping case results in an admissible curve (curve A–D–B), the overlapping forms an admissible area adjoined by curve A–D–B. The most linear approximation point is at C, which corresponds to $x_1 = 1$ and $x_2 = 0$. It has LAI = 0.959 and NVI = 0.0908.

ACKNOWLEDGMENT

The authors would like to thank P. LeFevre and E. Nesbitt for their editorial assistance. They would also like to thank the anonymous referees whose comments have greatly improved the presentation of this paper.

REFERENCES

- [1] K. J. Åström and T. Hägglund, "Automatic tuning of simple regulators with specification on phase and amplitude margins," *Automatica*, vol. 20, pp. 645–651, 1984.
- [2] K. J. Åström and B. Wittenmark, *Adaptive Control*, 2nd ed. Reading, MA: Addison-Wesley, 1995.
- [3] F. Bouslama and A. Ichikawa, "Fuzzy control rules and their natural control laws," *Fuzzy Sets Syst.*, vol. 48, pp. 65–86, 1992.
- [4] M. Braae and D. A. Rutherford, "Theoretical and linguistic aspects of fuzzy logic controller," *Automatica*, vol. 15, pp. 553–577, 1979.
- [5] C.-L. Chen and F.-C. Kuo, "Design and analysis of a fuzzy logic controller," *Int. J. Syst. Sci.*, vol. 26, pp. 1223–1248, 1995.
- [6] P. K. Dash and A. C. Liew, "Anticipatory fuzzy control of power systems," *Proc. Inst. Elect. Eng.—Gener. Transm. Distrib.*, vol. 142, pp. 211–218, 1995.
- [7] C. W. de Silva, *Intelligent Control, Fuzzy Logic Applications*. Boca Raton, FL: CRC, 1995.
- [8] R. C. Dorf and R. H. Bishop, *Modern Control Systems*, 7th ed. Reading, MA: Addison-Wesley, 1995.
- [9] D. Driankov, Hellendoorn, and M. Reinfrank, *An Introduction to Fuzzy Control*, 2nd ed. New York: Springer-Verlag, 1996.
- [10] D. E. Goldberg, *Genetic Algorithms in Search, Optimization, and Machine Learning*. Reading, MA: Addison-Wesley, 1989.

- [11] B. P. Graham and R. B. Newell, "Fuzzy adaptive control of a first-order process," *Fuzzy Sets Syst.*, vol. 31, pp. 47–65, 1989.
- [12] C. J. Harris, C. G. Moore, and M. Brown, *Intelligent Control, Aspects of Fuzzy Logic and Neural Nets*. London, U.K.: World Scientific, 1993.
- [13] A. Hasaon, P. Gruber, and J. Tödttli, "Fuzzy anti-reset windup for PID controllers," *Contr. Eng. Practice*, vol. 2, pp. 389–396, 1994.
- [14] S.-Z. He, S. Tan, F.-L. Xu, and P.-Z. Wang, "Fuzzy self-tuning of PID controllers," *Fuzzy Sets Syst.*, vol. 56, pp. 37–46, 1993.
- [15] J.-S. R. Jang, "Self-learning fuzzy controllers based on temporal back propagation," *IEEE Trans. Neural Networks*, vol. 3, pp. 714–723, 1992.
- [16] J.-S. R. Jang and N. Gulley, *Fuzzy Logic Toolbox User's Guide*. Natick, MA: Math Works, 1995.
- [17] J. Kim, Y. Moon, and B. P. Zeigler, "Designing fuzzy net controllers using genetic algorithms," *IEEE Contr. Syst. Mag.*, pp. 66–72, June 1995.
- [18] C. C. Lee, "Fuzzy logic in control systems: Fuzzy logic controller—Part 1 and Part 2," *IEEE Trans. Syst., Man, Cybern.*, vol. 20, pp. 404–435, 1990.
- [19] J. Lee, "On methods for improving performance of PI-type fuzzy logic controllers," *IEEE Trans. Fuzzy Syst.*, vol. 1, pp. 298–301, Feb. 1993.
- [20] Y. F. Li and C. C. Lau, "Development of fuzzy algorithms for servo systems," *IEEE Contr. Syst. Mag.*, pp. 65–72, Apr. 1989.
- [21] D. A. Linkens and H. O. Nyongesa, "Genetic algorithms for fuzzy control, part 1: Offline system development and application," *Proc. Inst. Elect. Eng.—Control Theory Appl.*, vol. 142, pp. 161–176, 1995.
- [22] D. A. Linkens and H. O. Nyongesa, "Genetic algorithms for fuzzy control, part 2: Online system development and application," *Proc. Inst. Elect. Eng.—Control Theory Appl.*, vol. 142, pp. 177–185, 1995.
- [23] H. A. Malki, H. Li, and G. Chen, "New design and stability analysis of fuzzy proportional-derivative control systems," *IEEE Trans. Fuzzy Syst.*, vol. 2, pp. 245–254, 1994.
- [24] E. H. Mamdani, "Application of fuzzy algorithms for simple dynamic plant," *Proc. Inst. Elect. Eng.*, vol. 121, pt. D, pp. 1585–1588, 1974.
- [25] V. S. Manoranjan, A. de S. Lazaro, D. Edwards, and A. Athalye, "A systematic approach to obtaining fuzzy sets for control systems," *IEEE Trans. Syst., Man, Cybern.*, vol. 25, pp. 206–213, 1995.
- [26] F. Matía, A. Jiménez, R. Galán, and R. Sanz, "Fuzzy controllers: Lifting the linear-nonlinear frontier," *Fuzzy Sets Syst.*, vol. 52, pp. 113–128, 1992.
- [27] M. Mizumoto, "Realization of PID controls by fuzzy control methods," *Fuzzy Sets Syst.*, vol. 70, pp. 171–182, 1992.
- [28] S. Murakami and M. Maeda, "Automobile speed control system using a fuzzy logic controller," in *Industrial Applications of Fuzzy Control*, M. Sugeno, Ed. Amsterdam, The Netherlands: North-Holland, 1985, pp. 105–124.
- [29] R. Palm, "Robust control by fuzzy sliding mode," *Automatica*, vol. 30, pp. 1429–1437, 1994.
- [30] D. Park, A. Kandel, and G. Langholz, "Genetic-based new fuzzy reasoning models with application to fuzzy control," *IEEE Trans. Syst., Man, Cybern.*, vol. 24, pp. 39–47, 1994.
- [31] X.-T. Peng, S.-M. Liu, T. Kamakawa, P. Wang, and X. Liu., "Self-regulating PID controllers and its applications to a temperature controlling process," in *Industrial Applications of Fuzzy Control*, M. Sugeno, Ed. Amsterdam, The Netherlands: North-Holland, 1985, pp. 355–364.
- [32] T. J. Procyk and E. H. Mamdani, "A linguistic self-organizing process controller," *Automatica*, vol. 15, pp. 15–30, 1979.
- [33] S. J. Qin and G. Borders, "A multiregion fuzzy logic controller for nonlinear process control," *IEEE Trans. Fuzzy Syst.*, vol. 2, pp. 74–81, Feb. 1994.
- [34] W. Siler and H. Ying, "Fuzzy control theory: The linear case," *Fuzzy Sets Syst.*, vol. 33, pp. 275–290, 1989.
- [35] M. Sugeno, "An introductory survey of fuzzy control," *Inform. Sci.*, vol. 36, pp. 59–83, 1985.
- [36] K. Tanaka and M. Sugeno, "Stability analysis and design of fuzzy control systems," *Fuzzy Sets Syst.*, vol. 45, pp. 135–156, 1992.
- [37] Q. H. Wu and B. W. Hogg, "On-line evaluation of auto-tuning optimal PID controller on micromachine system," *Int. J. Contr.*, vol. 53, pp. 751–769, 1991.
- [38] J.-X. Xu, C. Liu, and C. C. Hang, "Tuning of fuzzy PI controllers based on gain/phase margin specifications and ITAE index," *ISA Trans.*, vol. 35, pp. 79–91, 1996.
- [39] H. Ying, W. Siler, and J. J. Buckley, "Fuzzy control theory: A nonlinear case," *Automatica*, vol. 26, pp. 513–520, 1990.
- [40] H. Ying, "A nonlinear fuzzy controller with linear control rules is the sum of a global two-dimensional multilevel relay and a local nonlinear proportional-integral controller," *Automatica*, vol. 29, pp. 499–505, 1993.
- [41] Z.-Y. Zhao, M. Tomizyoshi, and S. Isaka, "Fuzzy gain scheduling of PID controllers," *IEEE Trans. Syst., Man, Cybern.*, vol. 23, pp. 1392–1398, 1993.
- [42] M. Zhuang and D. P. Atherton, "Automatic tuning of optimum PID controllers," *Proc. Inst. Elect. Eng.—Control Theory Appl.*, vol. 140, pp. 216–223, 1993.



Baogang Hu (M'94–SM'99) received the M.S. degree from the University of Science and Technology, Beijing, China in 1983, and the Ph.D. degree from McMaster University, Hamilton, ON, Canada in 1993, all in mechanical engineering.

He worked as a Lecturer at the University of Science and Technology, Beijing, from 1983 to 1987. In 1993, he was with NEFAB Inc., Canada. From 1994 to 1997, he was a Research Engineer and Senior Research Engineer at Center for Cold Ocean Resources Engineering (C-CORE), Memorial University of Newfoundland, St. John's, Nfld., Canada. Since 1997, he has been an Associate Professor at the National Laboratory of Pattern Recognition, Institute of Automation, Chinese Academy of Sciences, Beijing. His current research interests are in the areas of intelligent systems, pattern recognition, and plant growth modeling.



George K. I. Mann received B.Sc. (honors) degree in engineering from the University of Moratuwa, Sri Lanka, the M.Sc. degree in computer integrated manufacture from Loughborough University of Technology, U.K., in 1989, and the Ph.D. degree in 1999 from Memorial University of Newfoundland, St. John's, NFLD, Canada.

He is presently a Research Engineer in the Intelligent Systems Group, C-CORE, Memorial University, Newfoundland. Before he came to Canada he worked as a Lecturer, Department of Mechanical Engineering, University of Moratuwa, Sri Lanka. His research interests include classical/intelligent control and industrial automation.



Raymond G. Gosine (M'90) received the B.Eng. degree from the Memorial University of Newfoundland, St. John's, NFLD, Canada, in 1986, and the Ph.D. degree from Cambridge University, Cambridge, U.K., in 1990.

From 1990 to 1991, he was a Research Associate in engineering at the University of Cambridge and a Bye-Fellow of Selwyn College, Cambridge. From 1991 to 1993 he was the NSERC Junior Chair of Industrial Automation and an Assistant Professor, Department of Mechanical Engineering, University of British Columbia, Vancouver, BC, Canada. He is now an Associate Professor of engineering at Memorial University of Newfoundland and is the Director of Intelligent Systems at Center for Cold Ocean Resources Engineering, C-CORE, St. John's, Newfoundland. His research interests are in the area of industrial automation.